Bulletin of the Seismological Society of America, 90, 1, pp. 73–85, February 2000

Multiple Large Earthquakes in the Past 1500 Years on a Fault in Metropolitan Manila, the Philippines

by Alan R. Nelson, Stephen F. Personius, Rolly E. Rimando, Raymundo S. Punongbayan, Norman Tuñgol, Hannah Mirabueno, and Ariel Rasdas

Abstract The first ^{14}C-based paleoseismic study of an active fault in the Philippines shows that a right-lateral fault on the northeast edge of metropolitan Manila poses a greater seismic hazard than previously thought. Faulted hillslope colluvium, stream-channel alluvium, and debris-flow deposits exposed in trenches across the northern part of the west Marikina Valley fault record two or three surface-faulting events. Three eroded, clay-rich soil B horizons suggest thousands of years between surface faulting events, whereas ^{14}C ages on detrital charcoal constrain the entire stratigraphic sequence to the past 1300–1700 years. We rely on the ^{14}C ages to infer faulting recurrence of hundreds rather than thousands of years. Minimal soil development and modern ^{14}C ages from colluvium overlying a faulted debris-flow deposit in a nearby stream exposure point to a historic age for a probable third or fourth (most recent) faulting event.

Introduction

The economic and human loss resulting from recent damaging earthquakes in Northridge, California (U.S. Geological Survey, 1996), and Kobe, Japan (Holzer, 1995) highlight the need for evaluating potentially active crustal faults in urban areas (e.g., Dolan *et al.,* 1997). Manila—with a metropolitan population of about 10 million—is subject to shaking from earthquakes on nearby crustal faults as well as on more distant plate-boundary faults (Fig. 1a). The city has been heavily damaged by earthquakes at least six times in the past 400 years (Repetti, 1946; Garcia *et al.,* 1985), but specific sources for the earthquakes are uncertain. The Marikina Valley fault system, on the northeastern edge of the Manila metropolitan area (Figs. 1b and 2, Metro Manila), is a likely source for one or more of these earthquakes. Knowledge of the recurrence of large earthquakes on these crustal faults is needed to estimate the strength and probability of future earthquake ground motions in the metropolitan area (Thenhaus *et al.,* 1994).

Over the past three decades, detailed stratigraphic studies of sediments displaced by recent faulting have become a standard means of reconstructing the magnitude and recurrence of past earthquakes on surface-rupturing faults (Serva and Slemmons, 1995; McCalpin, 1996; Yeats and Prentice, 1996). Unfortunately, such fault assessment techniques have rarely been applied in the rapidly growing urban areas of developing countries. In the Philippines, interest in seismic hazard assessment was stimulated by the 1990 *M* 7.8 earthquake in northern Luzon (Punongbayan *et al.,* 1995; Fig. 1A). Daligdig *et al.* (1994) trenched scarps raised during this earthquake to determine the history of earthquakes on that branch of the Philippine fault system. Punongbayan *et al.* (1996) found evidence of recent lateral and thrust (?) movement in a trench across the east Marikina Valley fault (Fig. 2), but the absence of datable material precluded estimating earthquake recurrence on the fault.

Here we report the first radiocarbon-based earthquake recurrence estimate on a hazardous fault in the Philippines—the westernmost fault in the Marikina Valley system, about 10 km east of central Manila (Fig. 2). Stratigraphy, soil development, and ^{14}C data obtained from trenches and streambank exposures at the Maislap trench site show that a northern splay of the west Marikina Valley fault (Fig. 2) produced at least two and possibly four large earthquakes in the past 1300–1700 years. (Detailed logs of trench exposures, tables of lithologic data, and descriptions and interpretations of less important exposures are available as a downloadable electronic supplement (pdf format) to this article on the Seismological Society of America web site (*www.seismosoc.org*). In the text of the article, references to figures and tables in the supplement are preceded with an "S".)

Tectonic Setting

The Marikina Valley is a pull-apart basin bounded by the escarpments of the east and west Marikina Valley faults (Figs. 1b and 2). Smith (1924) and Alvir (1929) recognized that the valley was a graben formed by repeated fault move-

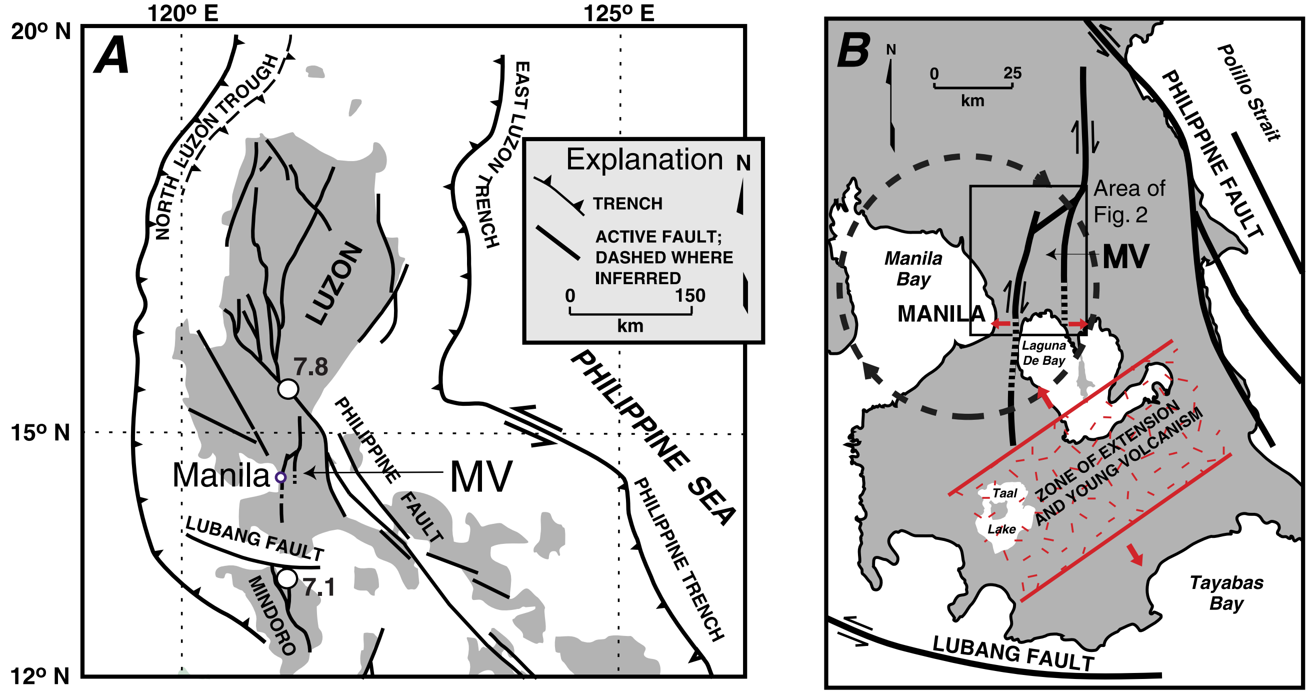

Figure 1. Tectonic setting of the Marikina Valley fault system (MV) in central Luzon, the Philippines. Diagram A shows subduction zone trenches by barbed lines, other faults with high rates of Quaternary activity by heavy black lines. White dots show locations of recent earthquakes on the Philippine fault in Luzon (*M* 7.8; 1990) and the Aglubang River fault in Mindoro (*M* 7.1; 1994). Diagram B shows how the Marikina Valley pull-apart basin (MV) may have been formed through extension caused by clockwise rotation (dashed circle) and shearing of central Luzon, which is caught between two active left-lateral strike-slip faults—the Philippine fault (Nakata *et al.*, 1977; Barrier *et al.*, 1991; Ringenbach *et al.*, 1993; Aurelio *et al.*, 1993) and the Lubang fault. A zone of extension and young volcanism south of the fault system has also influenced the structural development of the valley (Förster *et al.*, 1990; Defant *et al.*, 1988).

ments. Irving (1947) argued that primary fault movement was down-to-the-west in the northern part of the valley and down-to-the-east in the southern part. More complex movement histories were suggested by Gervasio (1968), who thought that the graben formed prior to strike-slip movement on the west Marikina Valley fault, and by Arcilla (1983) and Arcilla *et al.* (1989), who inferred that thrust and strike-slip faulting occurred before development of the graben. Right-lateral movement of the west and east Marikina Valley faults suggests clockwise rotation of the fault block underlying the valley (Fig. 1b). Block rotation may be caused by left-lateral strike-slip movement on the much larger Philippine fault in east central Luzon and on the Lubang fault between Luzon and Mindoro (Fig. 1a; Rimando *et al.*, 1995).

Landforms indicative of latest Pleistocene and Holocene strike-slip faulting, such as offset stream terraces and shutter ridges, are widespread along the traces of the east and west Marikina Valley faults north of the Pasig River (Punongbayan *et al.*, 1996; Fig. 2). Some of the most distinct right-laterally offset landforms lie along a northeast-trending trace of the west Marikina Valley fault in the northern part of the valley (Rimando *et al.*, 1995).

Both early and more recent investigators suggest that the west Marikina Valley fault may extend south of the Marikina Valley along the west side of Laguna de Bay as far south as Taal Lake (Fig. 1b; Gervasio, 1968; Förster *et al.*, 1990; Punongbayan *et al.*, 1996). A zone of extension northeast of Taal Lake (Fig. 1b; Wolf and Self, 1983; Defant *et al.*, 1988; Förster *et al.*, 1990) may also influence the fault. For example, continuing extension may explain the 10- to 100-m-high vertical scarps along the southernmost part of the west Marikina Valley fault where it intersects the zone.

Fault Exposures at the Maislap Site

Geology and Geomorphology

The Maislap site, in barangay (village-level political unit) San Isidro, is in the widest part of a narrow (50-m wide) strike valley on a northeastern splay of the west Marikina Valley fault, about 6 km north of Rodriguez (Fig. 2). Takashi Nakata and R.E. Rimando (written communication, 1994) identified the site during their 1991 mapping of the fault on topographic base maps (1:10,000 scale) using aerial photo-

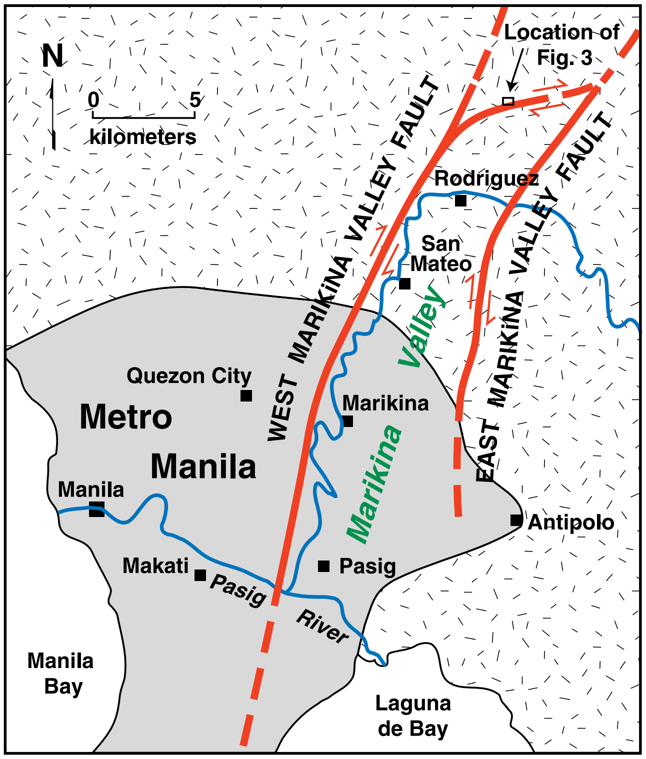

Figure 2. Location of the east and west Marikina Valley faults, which strike through the metropolitan Manila area (Metro Manila, light shading) of central Luzon. The Maislap trench site (Fig. 3) is on a northeast-trending splay of the west Marikina Valley fault north of the town of Rodriguez.

graphs (1:15,000 scale). A southeast flowing stream valley is offset right-laterally across the valley about 75 m near the trenches (tributary 1, Fig. 3). The channel of a larger stream and several adjacent fluvial terraces are also offset right-laterally at least 100 m about 1.1 km southwest of the site.

We selected the Maislap trench site from seven candidate sites for several reasons—the strike valley contains depressions where organic material for ^{14}C dating might be preserved, the valley is sufficiently narrow (<50 m) to trench completely across it to find the most recent trace of the fault, the site is in a relatively undisturbed agricultural rather than a developed area, there is good access for a backhoe, and the landowner is very cooperative and interested in our work.

We identified three traces of the fault (Fig. 3). Scarps that might have marked vertical displacements on fault traces have been obscured by logging and the construction of rice paddies beginning in the early 1970s. Nakata (written communication, 1994) inferred that a 1-m-high riser on the paddy terraces is a remnant of a former scarp that crossed the distal part of the colluvial apron extending southeastward from the small valley of tributary 2 near trench 1. Trenches 1 and 2 (inset A, Fig. 3) confirm the presence of the fault formerly marked by the scarp. Based on the projection of fault planes in stream exposures, two other fault traces parallel the valley northeast of the trenches. The heights of two small scarp remnants, 1 m and 32 m southwest of the longer stream exposure, suggest about 0.3 m of vertical separation along the northern trace. Exposures of bedrock against deformed, organic-rich colluvium and several springs suggest another recent trace on the northwest edge of the valley (See Part 3 of the electronic supplement to this article).

In order to decipher the history of surface faulting at the Maislap site, in the following sections we discuss the stratigraphy, structure, and age of sediments in two separate walls of trench 1, dug parallel to each other about 1.5 m apart (inset A, Fig. 3). We term the northeast wall of the initial trench wall 1 (Figs. 4a and S2 through S6) and the second wall, dug after study of the first wall was complete, wall 2 (Figs. 4b and S7). Stream channel and overlying colluvial deposits in these two walls are grouped into three depositional sequences of stratigraphic units bounded by erosional unconformities and/or soils that indicate periods of landscape stability (e.g., Kelsey *et al.*, 1998), labeled 1a, 1b, 2, and 3 on Figures 4, 6, and 7.

Estimating Ages of Stratigraphic Units

Our estimate of the age of the stratigraphic sequence at the Maislap site obtained from radiocarbon dating is three to nine times younger than the age suggested by the degree of soil development on the stream-channel deposits, debris-flow deposits, and colluvium exposed in the trenches. Here we outline the contrasting evidence for sequence age from radiocarbon dating and soil development and the reasons why we rely on ^{14}C for dating the stratigraphic sequence. We hope this explanation of age uncertainties early in the article will reduce confusion about our interpretation of ages in the following stratigraphy sections of the article. Most ^{14}C samples (Table 1; Figs. 4 and 5) consist of detrital charcoal and, therefore, their ages are maximums for their host sediment. We did not measure or directly calibrate the rate of soil development on stratigraphic units using ^{14}C or any other numerical dating method. Furthermore, many soil horizons are hard to interpret because they have been partially eroded or engulfed by younger overlying soils. Nevertheless, we estimated the times of surface-faulting events at the site by considering the maximum (14 samples) and minimum (four samples) age constraints provided by ^{14}C ages and the position of remnants of clay-rich soil horizons within the stratigraphic sequence. The primary age constraints are that (1) six of seven ^{14}C ages from the oldest units are between 1.3 and 1.7 ka, suggesting a young age of not much greater than this for the base of the exposed sequence, and (2) at least three separate, reddish, clay-rich soil horizons have formed within the sequence since the oldest units were deposited.

Radiocarbon Dating. We dated 19 of 48 samples of charcoal fragments collected from the exposures (triangle symbols on Figs. 4, 5, and S3 through S12) using accelerator

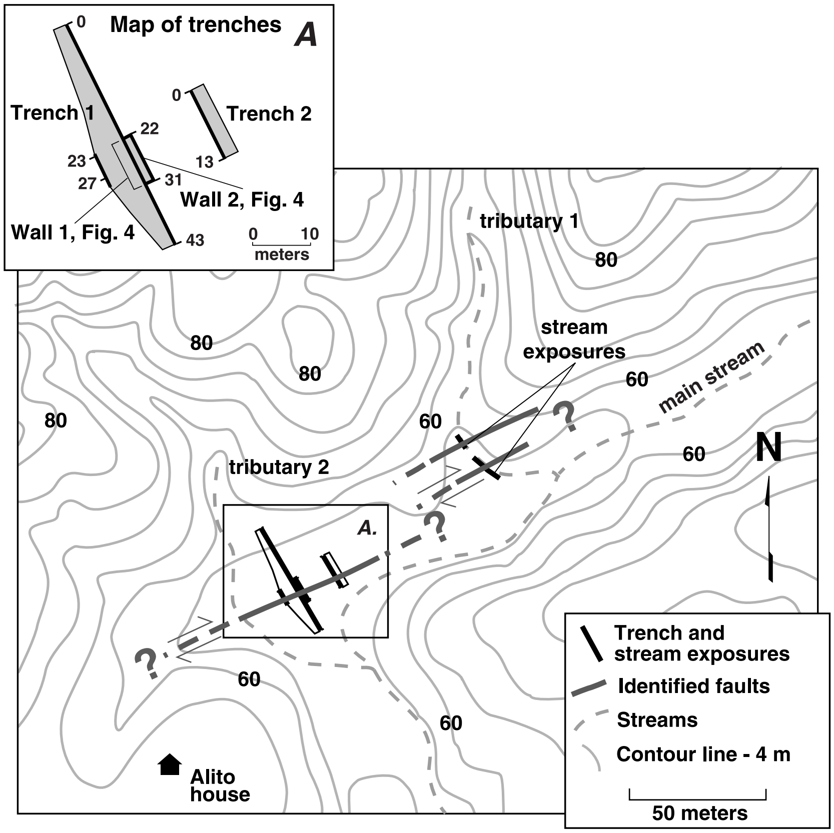

Figure 3. Map of the Maislap trench site, showing topography (4-m contour interval from Hacienda Remedios Sheet No. 3230-IV-23 1:10,000 topographic map, 1987), fault traces, and trench and stream exposures. Bold numbers on contours are elevation above sea level in meters. Inset A shows the location of mapped walls in trenches 1 and 2 (heavy lines); the floor of each trench is shaded. Numbers next to trench walls on A are station numbers as shown on maps of trench walls (Fig. 4 and Figs. S2 through S12 in the supplement to this article). Wall 2 of trench 1 was dug about 1.5 m northeast of wall 1 after description and sampling of wall 1 was complete. Trench 2 and all but the central part of trench 1 (wall 1 and wall 2 on Fig. 4) provide little definitive information about faulting; these exposures are discussed in the electronic supplement to this article.

mass spectrometer ^{14}C methods (Table 1). All samples were fragile, and several disintegrated during cleaning. Dated samples had ^{13}C/^{12}C ratios typical of woody and herbaceous land plants (-25.5 to -28.1‰ per thousand). We use two formats for ^{14}C ages (data in Table 1): to avoid clutter on Figures 4 and 5 and in the text, ages are abbreviated with "ka" (thousands of ^{14}C years B.P.), whereas in Figure 6 ages are calibrated and expressed as time intervals in calibrated (approximate solar) years A.D.

The size and distribution of charcoal fragments and some stratigraphically inverted ages on Figures 4 and 5 suggest that most of the fragments were washed down hillsides or carried by streams to the trench site. For example, we obtained ages of 1.6 ka and 1.7 ka from the oldest colluvial unit, but our oldest age (1.8 ka.) is from one of the youngest units in trench 1 (samples 1, 2, and 11, Fig. 4a). In contrast, several samples with anomalously young ^{14}C ages are either the remains of burned roots or are plant parts that were later incorporated into sediment filling burrows that we did not recognize when collecting the samples (Table 1). However, six of the 19 dated ^{14}C samples come from stratified units whose bedding is not disrupted by burrowing. The extent to which these ages constrain the times of faulting is discussed in the stratigraphy and chronology sections.

Degree of Soil Profile Development. The degree of argillic (clay-rich) soil horizon development (e.g., Birkeland, 1999) in stratigraphic units at the Maislap site is much greater than we would have expected for soils developed on sediments overlying colluvium dating from 1.3–1.7 ka. Two of three depositional sequences of stream channel deposits (Fig. 4) contain eroded, 15- to 40-cm-thick, argillic horizons (sandy clay loam and sandy clay textures) with translocated reddish-brown clay lining pores and coating highly weathered clasts. In parts of these horizons reddish-brown clay completely, engulfs grains of sand and silt. Many of the abundant, 4- to 15-mm-diameter mafic pebbles (derived from Cretaceous ophiolites, Arcilla *et al.*, 1989) in these horizons are completely weathered. Although some of the clay in these horizons may have been introduced through the erosion and transport of clasts from older argillic horizons upslope, widespread in-place translocated clay suggests that these horizons record thousands of years of landscape stability. A third, thicker (70 cm), less strongly developed, argillic horizon is developed in the silty, sandy colluvium of sequence 3. Because datable charcoal was common in many stratigraphic units and time for study of trench walls was limited, we chose detailed study of fault strands over detailed description of clay-rich soils.

Our mapping of the argillic horizons combined with the ^{14}C ages (Fig. 4) imply unacceptably high rates of argillic horizon formation. Although few radiocarbon ages are available, many similar clay-rich, alluvial soils in similar landscape positions in climates like those of Luzon (MAT of 28°C, MAP of 2.2 m) are thought to be several thousands

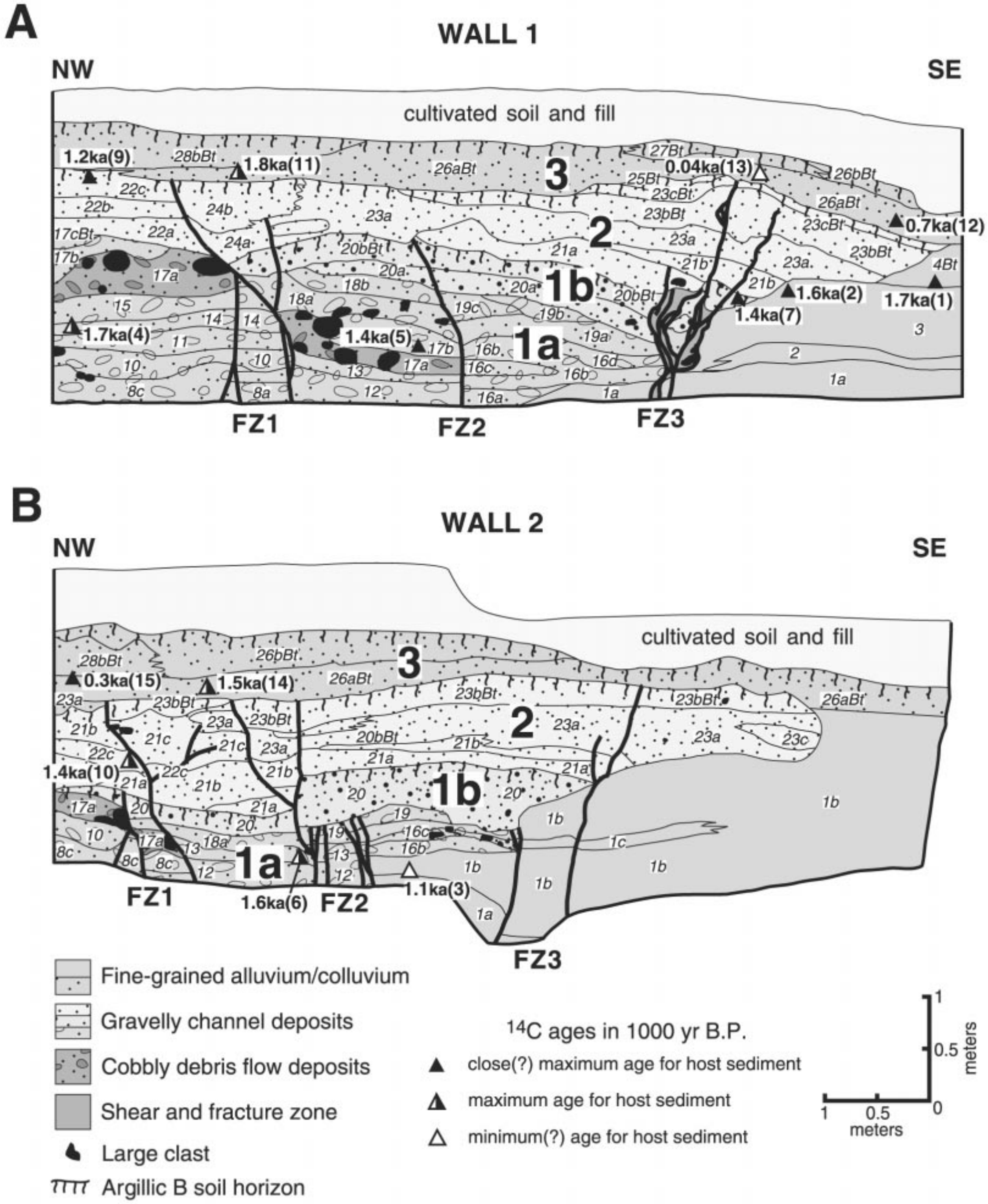

Figure 4. Simplified logs of the central parts of northeast wall 1 (a) and northeast wall 2 (b) of trench 1 at the Maislap site (inset A, Fig. 3; logged at a scale of 1:10). To avoid clutter, only the larger or more important stratigraphic units are labeled (italics). Subunits, designated a, b, c, or d, show different lithologic facies of a unit; Bt marks units that are largely remnants of argillic B soil horizons (B soil horizon symbols do not indicate horizon thickness). Heavy, shaded lines are fault traces and triangles show the location of charcoal samples collected for ^{14}C dating. Filled triangles mark detrital charcoal samples that are probably less than a few hundred years older than the enclosing sediment (close maximum ages based on our interpretation of the complete stratigraphic sequence); half-filled triangles mark samples that are probably at least a few hundred years older than the host sediment (maximum age); unfilled triangles show charcoal samples that are probably burned roots or charcoal incorporated into sediment filling animal burrows (minimum age). Numbers next to sample symbols are ^{14}C ages in thousands of ^{14}C years B.P. (ka), followed by the sample number on Table 1 in parentheses. The large numbers and progressively lighter shading show sequences (1a, 1b, and 2) of stream-channel and colluvial deposits of similar age that were faulted during two to three earthquakes (events A?, B and C, Fig. 6).

Table 1

Radiocarbon Ages from the Maislap Site

Sample Number	Stratigraphic* Unit	Stratigraphic* Wall	Description of Dated Material†	Sample Weight (mg)‡	Lab-Reported Age (^{14}C yr B.P.)	Calibrated Age (cal yr A.D.)§	^{13}C (‰ per thousand)	^{14} Laboratory Number
Oldest Colluvium								
1	4Bt	1	Five large fragments within sediment	10 est	1656 ± 51	244–551	−27.8	GX-20937
2	3	1	One 5×10-mm fragment	84.8	1580 ± 51	346–630	−25.7	GX-20934
3	1b	2	Highly decomposed fragments and dark clayey laminae	<5 est	1101 ± 45	[791–1027]	26.4	GX-20943
Sequence 1a								
4	14	1	One 4×4-mm fragment	35.2	1647 ± 46	(253–549)	−25.9	GX-20935
5	17b	1	One 3×5-mm fragment	15.5	1354 ± 41	601–789	−27.5	GX-20938
6	13	2	One large rounded brown clast and a few tiny fragments	<5? est	1615 ± 50	263–602	−27.1	GX-21222
Sequence 1b								
7	20bBt	1	Highly decomposed fragments broken into tiny frags	3 est	1366 ± 49	558–810	−25.5	GX-20932
8	9a	SW	Many large, highly decomposed fragments	20 est	1530 ± 49	(420–645)	−22.8	GX-20942
Sequence 2								
9	22c	1	Two 2×3-mm fragments broken into many pieces	<5? est	1160 ± 45	722–1010	−25.7	GX-21217
10	22c	2	One 3×4-mm fragment	<5? est	1390 ± 50	(545–781)	−28.6	GX-21221
Sequence 3								
11	26aBt	1	Three 2×3mm fragments	36 est	1825 ± 43	(77–371)	−26.6	GX-20936
12	26aBt	1	Small fragments in clayey sediment, has wood structure	<1 est	687 ± 41	1256–1400	−26.5	GX-20933
13	26aBt	1	One 0.5-mm-thick, 2–3-mm-long, decomposed seed pod?	30 est	40 ± 40	[1684–1932]	−27.8	GX-21218
14	26aBt	2	Six 0.5-mm dark clayey laminae, some with structure	10 est	1503 ± 59	(416–666)	−27.0	GX-20940
15	26aBt	2	Few tiny fragments broken from 3 2×3-mm fragments	<1 est	310 ± 90	1426–1954	−29.1	GX-21223
Stream Exposure								
16	9c		Two 5×6-mm fragments of wood charcoal	110 est	422 ± 40	1418–1634	−26.5	GX-20941
17	9b		Four 1×1-mm fragments, possibly roots	10 est	modern	[modern]	−24.0	GX-21220
18	6a		Six 2×4-mm fragments	15.6	120% of modern	[modern]	−28.1	GX-20939
19	11bB		Two 4×3-mm angular fragments, possibly a rootlet	45 est	145% of modern	modern	−27.2	GX-20931

*Location of samples on Figures 4, 5, and 6. More precise locations and the location of sample 16 on the southwest wall of trench 1 (Figure 59) are shown in the electronic supplement to this paper.

†Except as noted, all samples are angular fragments of detrital woody charcoal, which were cleaned in water at 60–120×.

‡Because many samples were so fragile, most sample weights are estimates (est). Many estimates are maximums because some sediment could not be removed during cleaning without destroying the sample. Sample 3 contained only about 0.05 mg of carbon (H. Krueger, oral commun., 1995).

§Calibrated at two standard deviations using the bidecadal data set and an interlaboratory error multiplier estimated at 1.3 (method of Stuiver and Reimer, 1993).

Ages in parentheses are probably on charcoal reworked from older units; these are maximum ages for the respective units. Ages in brackets are probably on rootlets or charcoal in filled burrows; therefore, these are minimum ages.

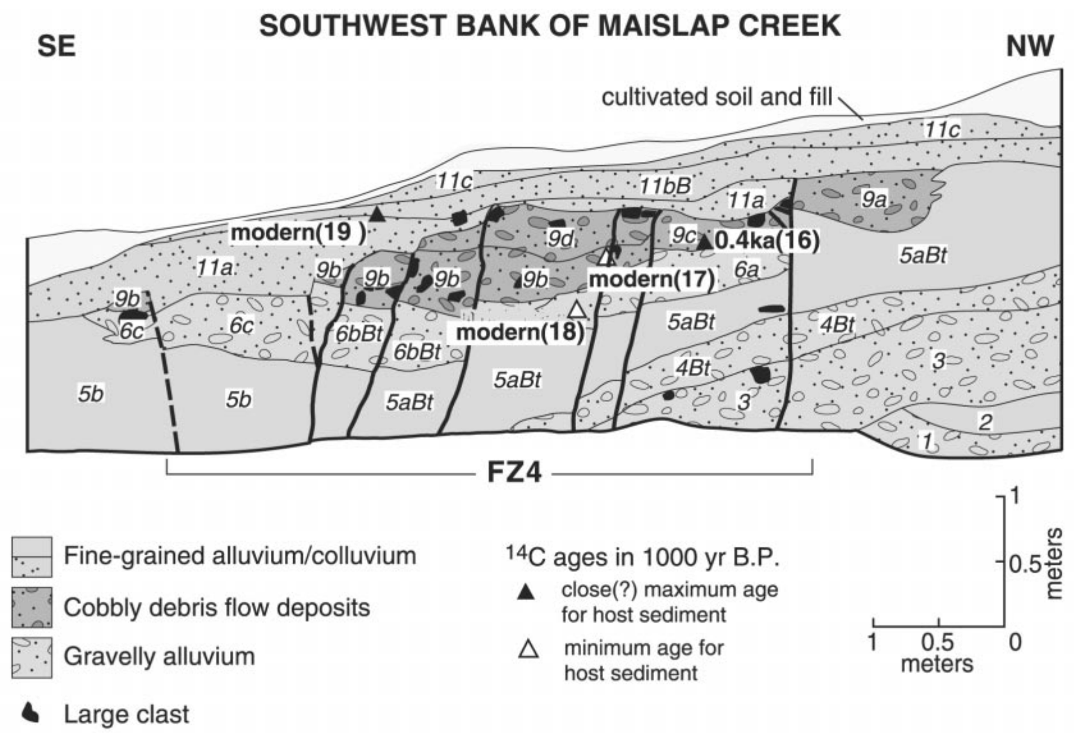

Figure 5. Simplified log of the central part of a 15-m-long natural stream bank exposure at the Maislap site (Fig. 3). Heavy lines are fault traces and triangles show the location of charcoal samples collected for ^{14}C dating (symbols and labels as on Fig. 4). In this exposure we found evidence for a probable fourth surface-faulting event D (Fig. 6).

of years old (e.g., Alexander and Holowaychuk, 1983; Bullard *et al.*,1988). Perhaps much of the clay in the horizons at the Maislap site was derived from older soils (e.g., Markewich *et al.*, 1988); clasts eroded from old, nearby argillic horizons and incorporated into younger soils may even retain their thick clay films. Nevertheless, the distribution of reddish clay films, weathered clasts, and yellow-orange sediment color (indicating iron oxidation) in these soils are typical of the lower B and C horizons of many strongly developed soils on landscapes that are thousands of years old.

Because there cannot have been thousands of years of soil development between soil horizons within a stratigraphic sequence dating from 1.7 ka, we are forced to choose between the radiocarbon ages and the characteristics of the buried soil horizons to estimate the age of the Maislap sequence. The ^{14}C samples were collected, selected, pretreated, and analyzed following rigorous standardized procedures; furthermore, 15 of the 19 ages are consistent with a sequence age of 1.7 ka. Soils data are much more limited and the eroded, discontinuous horizons are difficult to interpret. Although we cannot adequately explain the development of the argillic horizons between faulting events, stratigraphic and sedimentologic evidence prevents us from dismissing all ^{14}C ages as contaminated or from sediment-filled burrows (minimum ages). For this reason, we suggest that the argillic horizons mark periods of hundreds rather than thousands of years between the depositional sequences (1b, 2, and 3, Fig. 4) and acknowledge that we do not fully understand how they formed.

Stratigraphy of Trench 1, Wall 1

We dug trench 1 across the strike valley to locate the main trace of the west Marikina Valley fault (Fig. 3). A complex sequence of intertonguing colluvial and fine-grained alluvial stratigraphic units, some capped with eroded remnants of argillic B horizons (labeled Bt), slope gently into the valley in the northwest half of trench 1 (Figs. S2 and S3; only the middle quarter of trench 1 is shown in Fig. 4a). Most units consist of silty clay or clayey silt with some sand and a few weathered pebbles. In the lower half of the trench, about a third of the way toward its southeast end, the fine-grained units interfinger with coarse, gravelly, cobbly units that mark former channels of the main stream. Several of the more cobbly units are the remains of debris flows from the tributary 1 drainage (Fig. 3).

None of the stratigraphic units in the northwest half of trench 1 (Figs. S2 and S3; inset A, on Fig. 3) appear to be faulted, indicating that the most recent trace of the west Marikina Valley fault lies farther to the southeast. A possible

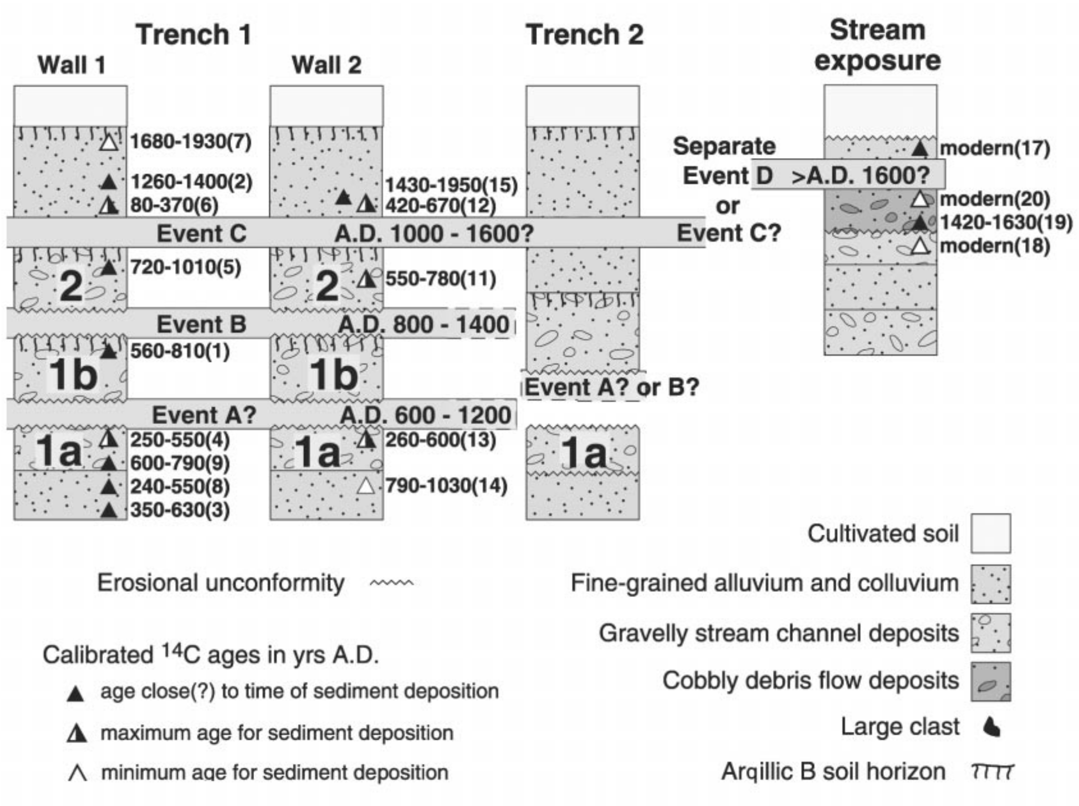

Figure 6. Diagram showing relations among stratigraphic units and timing of surface-faulting earthquakes at the Maislap site. Triangles show ^{14}C-dated charcoal samples as in Figure 4; ^{14}C ages are calibrated and expressed as time intervals in cal yr A.D. (approximate solar years A.D., Stuiver and Reimer, 1993) at two standard deviations and rounded to the nearest 10 years (Table 1). Large numbers correspond with sequences of stream-channel and colluvial deposits (sequences 1a, 1b, and 2) displaced during faulting events A?, B, and C, respectively. Erosional unconformities bounding deposits are inferred from truncated bedding and soil horizons. Question marks indicate uncertainty in the existence of event A, the stratigraphic position of events B and C in trench 2, and the age range of event C.

exception is a small, steeply dipping fault with about 20 cm of vertical displacement near the northwest end of the trench. The isolated occurrence of this fault, its position near the base of a steep hillslope, and its southeast dip suggest that it is part of the headscarp of an old landslide rather than a tectonic fault.

In the middle of trench 1, the gravelly deposits thicken and are displaced by fault strands concentrated in three zones (FZ1, FZ2, and FZ3 on Figs. 4, S4, S6, and S7). The gravelly deposits pinch out in the southeast quarter of the trench where the trench walls consist primarily of massive, fine-grained colluvium with thick Bt horizons and no evidence of faulting (Fig. S5). Indistinct outlines of animal burrows are common in some of these fine-grained units and in other similar colluvial units in trench 1. However, because there is so little contrast between the lithology of fine-grained colluvium and the sediment filling the burrows, it is difficult to assess the degree of mixing by burrowing in some parts of the trench, especially where Bt horizons have engulfed previously burrowed sediment. Two ^{14}C ages on pieces of wood charcoal from the middle of trench 1 suggest a maximum age for deposition of much of the colluvium of about 1.5–1.7 ka (samples 1 and 2, Fig. 4a and Table 1).

Wall 1 exposed three sequences of gravelly to cobbly stream-channel and debris-flow units (Fig. 4a) deposited in channels eroded by the stream into the older fine-grained colluvium and alluvium (units 1–4). The oldest channel deposits (sequence 1a, units 8–19) are cobbly with a few boulders in some units and are capped by a thick debris-flow deposit (unit 17a) near the northwest edge of Fig. 4a. We obtained ^{14}C ages of 1.7 ka and 1.4 ka on fragments of charcoal in the channel deposits (samples 4 and 5, Fig. 4a and Table 1). Because these fragments are older than the sediments that contain them, the channel deposits were deposited after 1.4 ka. As noted for similar samples by Lienkaemper and Borchardt (1996) and Kelson *et al.* (1996), the older age is clearly hundreds of years older than the channel deposits; the younger age may or may not be significantly older.

Another gravelly channel deposit (sequence 1b, unit 20, Fig. 4a) overlies those of sequence 1a. The lower contact of unit 20 is sharp and irregular, clearly indicating that it is erosional. Because there is no soil developed on units 17, 18, and 19, we cannot determine the length of time between deposition of sequence 1a and sequence 1b (unit 20). For this reason, we group all these units into sequence 1. The remains of a well-developed argillic horizon is preserved in the upper two-thirds of unit 20 suggesting that it is at least a few hundred years older than the overlying channel deposits of sequence 2 (units 21–25). The horizon (unit 20bBt) contains abundant reddish-brown infiltrated clay and 40–50% completely weathered basalt pebbles. The only ^{14}C age from unit 20 (sample 7 near FZ3) is about the same age (1.4 ka) as the younger of the two ages from sequence 1a. Thus, ^{14}C ages show that both sequence-1a and sequence-1b units are no older than this age.

Another sequence of fine gravelly channel deposits (sequence 2, Fig. 4a; units 21–25) with very distinct, planar fluvial bedding overlies sequence 1 (unit 20). An argillic horizon with abundant reddish-brown clay and 50–60% completely weathered pebbles is developed in the top of sequence 2 (units 23bBt, 23cBt, and 25Bt). Some of the weathering and clay accumulation could be the result of soil development on the younger overlying colluvium of sequence 3 (the Bt horizon beneath the cultivated soil, units 26–28). However, the sharp contact at the top of sequence 2 and the difference in clay content across the contact indicate that the channel deposits were not deeply buried by younger colluvium until a clay-rich soil had developed on them. A single age from near the top of unit 22c indicates that sequence 2 is younger than 1.2 ka (sample 9, Fig. 4a and Table 1).

From three ages on charcoal in the colluvium of sequence 3 in wall 1 (units 26–28) we infer an age for the sequence of less than 0.7 ka (sample 12, Fig. 4a). The oldest age of 1.8 ka (sample 11) must be from a piece of charcoal eroded from older deposits. The 20- to 70-cm-thick argillic horizon developed in sequence 3 suggests at least a few hundred years of soil development. Thus, the age of 0.04 ka (sample 13) from unit 26aBt is either from the remains of a small root that burned in place or a charcoal fragment incorporated into the sediment by animal burrowing. A layer of post-A.D. 1970 cultivated soil and fill more than half-a-meter thick overlies the young alluvium and colluvium along wall 1 in the middle of trench 1 (Fig. 4a).

The vertical extent of fault strands concentrated in the three fault zones (Fig. 4a) show that at least two surface faulting events are recorded in the sediments of wall 1 (events B and C, Figs. 6 and 7). Three strands in zones FZ2 and FZ3 terminate near the top of sequence 1b (unit 20); five other strands extend into sequence 2 (units 23 and 24), but only two reach its upper contact. Tracing individual fault strands within the narrow shear and fracture zone of the lower part of FZ3 is difficult. Several short indistinct strands may terminate at the top of sequence 1a (unit 19), but this is insufficient evidence to confirm a third, earliest faulting event (Fig. 7). However, the vertical displacement of unit 20 in the lower part of FZ3 and the absence of vertical displacement in the upper part suggest different styles of faulting during at least two events. Sequence 2 (units 21–25) in FZ3 appears to have been pushed upward into a dome shape. The dome shape and the upward-splaying pattern of fault strands are typical of strike-slip faults (Weldon *et al.*, 1996).

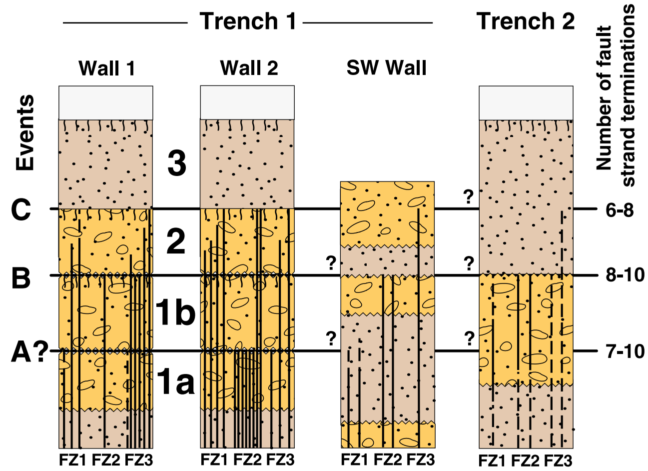

Figure 7. Vertical extent of fault strands (solid vertical lines) in fault zones relative to the stratigraphic position of surface faulting events A?, B, and C in trenches 1 and 2. Patterns, symbols, and labels for faulting events, stratigraphic sequences, and fault zones as in Figures 4 and 6. Indistinct or inferred parts of strands are dashed. The range in the number of terminations for each faulting event (right edge of figure) is the number of distinct strands and the total number of strands. Question marks indicate uncertainty in the correlation of faulting events to strands in the southwest wall of trench 1 and in trench 2. Although as many strands were mapped terminating near the position of event A? as for any other event (7–10), all but one of the distinct strands terminating at this position were in one fault zone (FZ2, wall 2). For this reason, we cannot demonstrate that event A? is a separate faulting event.

The largest measured separations in wall 1 include an apparent 75 cm of cumulative vertical separation of the upper contact of unit 17 in FZ1 and the 30 cm of vertical separation of the upper contact of unit 20 in FZ3 during faulting event B. Lateral displacements on the faults in wall 1 are difficult to estimate from a fault-perpendicular trench.

Stratigraphy of Trench 1, Wall 2

Wall 2 of trench 1 (Figs. 3 and 4b) had stratigraphy, soil development, and fault patterns very similar to those in wall 1. Most of the units in wall 1 are recognized in wall 2 and have the same unit numbers. The main differences in stratigraphy between the two walls are that unit 17a is thinner and units 20 and 21 are thicker in wall 2 than in wall 1. Overall, patterns of faulting differ only in that in wall 2, more fault strands are found in FZ2 than in wall 1 and the slight dome-like deformation of sequence 2 is farther to the northwest between FZ2 and FZ3.

The largest vertical separations measured in wall 2 are about 20–30 cm, across the upper contacts of units 1a in FZ3, unit 20 in FZ2, unit 17a in FZ1, and unit 22c in FZ1. Relations among the fault strand in FZ1 and units contacts suggest that the 20-cm separation of unit 22c occurred during faulting event C (Fig. 6). Other separations, however, especially the large vertical separations of 40 to 60 cm measured for units 21a and 21b, reflect uncertainties in mapping and correlating facies changes across fault strands, the probable nonplanar geometry of some units, and displacement during successive faulting events.

Wall 2 shows evidence of a possible third faulting event. Seven fault strands terminate at the top of sequence 1a (unit 19; Figs. 4b and 7) in wall 2, and the erosional unconformity at the top of sequence-1a is more distinct than in wall 1. However, all but one of the distinct strands are confined to a 0.5-m-wide zone in FZ2 (Fig. 7) and no soil, which would suggest an age difference between sequences 1a and 1b, is preserved at the top of sequence 1a. In strike-slip fault zones, upward terminations of fault strands must be widely distributed and occur consistently at the same stratigraphic contact to infer a faulting event at the contact (Weldon *et al.*, 1996). As the strands that terminate at the top of sequence 1a do not meet these criteria, we infer only that a third, earliest faulting event (event A?, Figs. 6 and 7) is likely but not demonstrated. Thus, the pattern of fault strands and stratigraphy exposed in the two walls of trench 1 show that at least two and possibly three faulting events have occurred in this part of the valley.

Three of the five ^{14}C ages from wall 2 are older than their host sediment, and one age seems anomalously young. Ages of 1.6 ka and 1.4 ka from sequences 1 and 2, respectively, and 1.5 ka from sequence 3 (Fig. 4b; samples 6, 10, and 14) are the same age or older than the youngest ages obtained from equivalent units in wall 1. An unusually young radiocarbon age of 1.1 ka (sample 3) from the oldest colluvium in wall 2 (unit 1b) is probably less accurate than the other ages because the amount of charcoal dated was very small (Table 1). Perhaps this sample was incorporated into sediment filling an unrecognized burrow younger than the surrounding colluvium. The younger of the two ages from the colluvium of sequence 3 in wall 2 is 0.3 ka (sample 15). Unless the dated charcoal was incorporated into sediment filling an unrecognized burrow, this age is probably a close maximum age for the colluvium at this depth.

Stratigraphy of Other Trench Exposures

Additional trench exposures at the Maislap site (Figs. 3 and 7; Part 3 of supplement) include: a 1.5-m-long, northeast-trending section connecting trench walls 1 and 2; a 5-m-long section of the southwest wall of trench 1; a second 13-m-long trench (trench 2) between trench 1 and the stream exposures; and a small hand-dug trench about 2 m southwest of the longer stream exposure. At least two faulting events were identified in the southwest wall of trench 1 and in trench 2. However, because we gained little additional information about faulting event timing or the amount of fault separation from these additional exposures, we relegate their descriptions to the electronic supplement to this paper.

Stratigraphy of the Stream Exposure

A 15-m-long section of steam bank about 63 m northeast of trench 2 (longer, southeasterly exposure on Fig. 3) exposed additional surface faulting. In the bank exposure, gravelly alluvium deposited from the tributary-1 drainage and fine-grained hillslope colluvium are interbedded and slope toward the southeast (Figs. 5, S11, and S12). Near the top of the exposure, a cobbly debris-flow deposit (unit 9) is displaced by several near-vertical faults. The most southeasterly fault strands abruptly terminate the tip of unit 9, probably displacing it toward the southwest (into the plane of Fig. 5). Cumulative separation across all the strands in unit 9 is about 30–40 cm, but at least some of this separation is probably the result of the nonplanar geometry of the debris-flow deposit. The small, indistinct vertical separations of only a few centimeters on the fault strands cutting units 3–5 do not suggest older displacement events.

The steeply dipping, subparallel pattern of the fault strands in the stream exposure is more typical of extensional faulting rather than the type of oblique-slip faulting inferred from the trenches. Deposits displaced by lateral spreading may also show extensional fault patterns. But we ruled out lateral spreading because (1) the faults were concentrated in 5-m-wide zone along the exposure that coincides with the remnant of a valley parallel scarp, (2) unconsolidated deposits here are thin (the stream flows on bedrock at the base of the exposure), (3) there is probably insufficient relief to facilitate spreading in this part of the valley, and (4) humic-rich soil that is probably less than a few hundred years old is faulted against bedrock in the other stream exposures 15 m to the northwest.

The lack of soil development on unit 9 and on the thin overlying unit of fine-grained colluvium (unit 11, Fig. 5) suggests that the faulted debris flow deposits are less than a few hundred years old. A weak cambic B horizon (unit 11bB) is barely recognizable on the unfaulted colluvium above unit 9; its degree of development is so much less than that of the B horizons developed in the similar deposits of sequence 3 in the trenches that it may be less than a century or two old. Burrowing has disturbed the B horizon and obscured the lower contact of unit 11 in places, but this unit is more consolidated and clearly older than the loose, organic-rich, cultivated soil and fill above it. A maximum ^{14}C age of 0.4 ka on a large angular piece of wood charcoal (sample 16, Table 1) confirms a young age for unit 9. A modern ^{14}C age from the overlying colluvium may be an accurate age (modern ages are interpreted as less than 150 years B.P., sample 19) for unit 11, but the two lower modern ages in unit 9 must be younger than the debris-flow deposit (samples 17 and 18). The modern-aged samples probably are either small burned roots or, more likely, charcoal that was incorporated into sediment filling animal burrows.

Chronology of Surface Faulting Events

Comparison of the stratigraphy in the walls of trench 1, the southwest wall of trench 2, and the logged stream exposure suggest that two to four large surface-faulting earthquakes occurred on the west Marikina Valley fault in the past 1300–1700 years. In the following discussion of the chronology of depositional, erosional, and faulting events we express calibrated ^{14}C ages (method of Stuiver and Reimer, 1993) as time intervals in calendar years A.D. (cal yr A.D.; Fig. 6 and Table 1). Because of large uncertainties about the length of the intervals between the times when the plants that produced the dated charcoal died and the times when charcoal-containing units were faulted (most ages are maximum ages for the times of faulting events; a few are minimums), we estimate only broad time ranges within which these earthquakes occurred. We interpret ages marked by half-filled triangles in Figure 6 (and within parentheses in Table 1) to be maximum ages at least a few hundred years older than the enclosing sediment. Therefore, we do not use these ages for estimating the times of faulting.

The first depositional event is the gradual deposition of the oldest, fine-grained colluvium and alluvium sometime after A.D. 240–630 (samples 1 and 2; Fig. 6). The sample 3 age (790–1030 cal yr A.D., Fig. 6) suggests deposition after about A.D. 800–1000, but because this sample contained a very small amount of carbon (Table 1) we have less confidence in this age than in the ages for samples 1 and 2. Most of this sediment was washed off steep hillsides, although some may have been carried down the valley during floods. Next, the stream shifted its position in the valley, eroded a channel into the colluvium, and deposited the sequence 1a channel deposits (Fig. 4), probably during several major floods. Following the deposition of sequence 1a after about A.D. 600–800 (sample 5), a surface-rupturing earthquake (event A?, Fig. 6) may have occurred, displacing sequence 1a in wall 1 and possible equivalent units in the southwest wall of trench 1 (Fig. S9). Based on the ^{14}C ages in sequence 1a deposits, this earthquake, if it occurred, is no older than about A.D. 600 (sample 5).

Next the stream cut down into sequence 1a and deposited more channel deposits (sequence 1b, Fig. 4). Some of the gravelly deposits in trench 2 may have been deposited at this time or may be younger. The stream channel then moved eastward away from the main traces of the fault, and a soil developed on the sequence 1b deposits. After at least a few hundred years of soil development, a surface-faulting earthquake (event B) displaced sequence 1 (1a and 1b) in all three fault zones in trench 1 and in one or two correlative zones in the southwest walls of trenches 1 and 2 (Figs. 7, S9, and S10). The single maximum ^{14}C age from sequence 1b (560–810 cal yr A.D., sample 7, Fig. 6) indicates that event B is younger than about A.D. 600. If event A is a separate, earlier faulting event, then event B occurred long enough after event A for the argillic horizon to develop on sequence 1b.

After event B, the stream returned to its former position and cut a new channel into sequence 1 and into the oldest fine-grained alluvium and colluvium (Fig. 4). Following laterally extensive deposition of gravel in the new stream channel, the stream shifted away from the trench site and a new argillic horizon developed on sequence 2. Gravelly channel deposits in trench 2 were probably deposited during this period. After the few hundred or more years needed for argillic horizon development, faulting event C (Fig. 6) displaced the channel deposits of sequences 1 and 2 in trenches 1 and 2. Radiocarbon ages for samples 9, 12, and 15 from trench 1 indicate that event C probably occurred after A.D. 720–1010 and before A.D. 1430–1950, and perhaps before A.D. 1260–1400. The argillic horizon on sequence 2 suggests event C occurred at least a few hundred years after event B.

Following event C, the fine-grained colluvium of sequence 3 was gradually deposited over sequence 2. A cumulic soil with a 20- to 70-cm-thick argillic horizon continued to develop in these and the underlying deposits until the valley floor was plowed and terraced for rice paddies in the early 1970s. The thick Bt horizon in the colluvium must have required at least a few hundred years to develop—a minimum estimate of the age of event C. We identified no faults in the post-event-C deposits in trench 1, although a possible younger faulting event may have displaced fine-grained colluvium in trench 2. Faults, however, are commonly indistinct in massive, fine-grained colluvium (e.g., Weldon *et al.*, 1996).

As shown on Figure 6, ^{14}C ages provide maximum constraints for the times of faulting events, but the constraints allow only hundreds of years for argillic horizon development between faulting events. We remain confused as to how three such horizons, which are interpreted as forming over thousands of years in similar climates, could develop in the 1500- to 1700-year interval since the oldest colluvium in trench 1 was deposited. For this reason, we refrain from using our "few hundred years" estimate of the minimum times needed for soil formation to calculate more precise estimates of the times of faulting events.

Faults that displace the debris-flow deposit in the central part of the logged stream exposure (Fig. 5; event D, Fig. 6), are probably younger than faulting event C in trench 1. The ^{14}C age on the large fragment of charcoal in the debris-flow deposits (sample 16) indicates deposition after A.D. 1420–1630. The absence of a distinct soil on the debris-flow deposit and the presence of only a weak cambic B horizon on the overlying unfaulted colluvium suggests that the debris flow was deposited after event C, perhaps during a major storm in the past century or two. Although no faulting younger than event C was recognized in trench 1, if distributed displacements on fault strands were less than a few centimeters during event D, such a faulting event might go unrecognized, especially in the complex alluvial/colluvial stratigraphy in the northwestern half of trench 1 (Figs. S2 and S3).

Our dating is obviously too imprecise, and intensity data for the historical earthquakes that struck Manila beginning in A.D. 1599 are too localized to correlate any historical earthquake with a particular faulting event on the west Marikina Valley fault. Nevertheless, because faulting event D probably occurred during the historic period, it probably corresponds with one of the earthquakes that shook Manila in A.D. 1599, 1601, 1658, 1700, 1766, or 1863 (historical accounts in Garcia *et al.,* 1985). If events C and D are not the same faulting event, one of the earliest of these earthquakes could possibly have caused event C.

Magnitude and Frequency of Large Earthquakes on the Marikina Valley Fault System

Based on our interpretation of exposures at the Maislap site, at least two and perhaps four surface-rupturing earthquakes have occurred on the northeastern splay of the west Marikina Valley fault since A.D. 600. This is a short interval of time relative to total errors in the ^{14}C dating of faulting events; all our ^{14}C ages are on detrital (transported) charcoal that provide only maximum or minimum constraints on the times of faulting. For this reason, we cannot determine the time of each faulting event or calculate precise earthquake recurrence intervals. Four surface-rupturing earthquakes over a period of less than 1300 years (the interval A.D. 600 to A.D. 1863) suggests average recurrence intervals of less than 500 years. But if only two earthquakes occurred (If A? and B are the same event, and C and D are the same event.), recurrence could be more than 1000 years.

We suggest a conservative range of 300 to 1000 years be used in assessing the hazard from surface-rupturing earthquakes on the northern part of the west Marikina Valley fault. Such a range reflects the uncertainty of our dating and the fact that recurrence data are available from only a single site. Both historic and detailed prehistoric records of large earthquakes illustrate that recurrence on individual faults is commonly clustered (e.g., McCalpin, 1996; Yeats and Prentice, 1996). However, the time intervals needed to form the three soils with argillic B horizons in trench 1 suggest earthquakes that were not tightly clustered in time. For this reason and because we think events C and D are separate events, we favor shorter recurrence intervals of roughly 400–600 years over longer intervals of 1000 years.

Estimates of the magnitude of prehistoric earthquakes are commonly based on fault rupture lengths and/or fault displacements (Wells and Coppersmith, 1994). Unfortunately, we cannot estimate the lateral component of fault displacement from the three fault-perpendicular exposures at the Maislap site. More trenches as well as offset landforms are required to accurately measure lateral-fault displacements, and it is not clear whether the stratigraphy at the site is suitable for such measurements.

We speculate that the vertical separations of 20 to 40 cm that occurred during individual surface-faulting events on the fault strands of Figures 4 and 5 reflect lateral slip of about 1–2 m during each event. Landforms (Punongbayan *et al.,* 1996) show that recent displacement on the west Marikina Valley fault is primarily right lateral, but the ratio of vertical to lateral displacement is unknown. If the ratio is similar to ratios (1:2 to 1:8) measured along scarps on the DigDig fault in northern Luzon after the *M* 7.8 1990 earthquake (Punongbayan *et al.,* 1995) and the Aglubang River fault in Mindoro after the *M* 7.1 1994 earthquake (PHIVOLCS Quick Response Teams, 1994; Fig. 1a), then the separations are consistent with earthquakes of *M* 6–7 (Wells and Coppersmith, 1994).

Empirical relations between rupture lengths and magnitudes of historic earthquakes in similar tectonic environments also imply earthquakes of *M* 6–7 on the Marikina Valley fault system. About 30 km of the northern half of the west Marikina Valley fault is marked by young, fault-related landforms (Punongbayan *et al.,* 1996), a fault length that corresponds with *M* 6–7 earthquakes. Although a much longer section of the fault (e.g., Gervasio, 1968; Förster *et al.,* 1990; Punongbayan *et al.,* 1996) possibly ruptured during earthquakes as large as *M* 7.5, landforms suggesting repeated rupture of the west Marikina Valley fault southward beyond the Pasig River have yet to be identified (Figs. 1b and 2). Fault-related landforms extend along an even shorter section (18-km long) of the east Marikina Valley fault, so the chance of an earthquake larger than *M* 7 on the faults of the Marikina Valley system seems small.

Acknowledgments

This project was conceived by S.T. Algermissen as part of the U.S. Geological Survey's Worldwide Earthquake Risk Management program. Algermissen also obtained funding for the project from the U.S. Agency for International Development, The Philippines (Technical Resources Project No. 492-0432). R.S. Punongbayan obtained further funding from the Philippine Department of Public Works and the insurance industry in Manila (primarily backhoe support, PHIVOLCS salaries, and supplies). We thank David Nelson and José Garzon of U.S. AID in Manila for being strong advocates of our work. Takashi Nakata (Hiroshima University, Japan) identified the Maislap trench site during earlier geomorphic mapping projects and encouraged us to trench it. Chris Newhall (USGS, Vancouver, Washington), and Donald Wells, Andy Thomas, and Tom Bullard (all with Geomatrix Consultants, San Francisco) gave valuable advice and loaned us equipment. Lee-Ann Bradley helped prepare Figures 1–5 and Tom Gardner, Roy Shelmon, Jim McCalpin, Carol Prentice, Michael Machette, Kathy Haller, Clarence Allen, and an anonymous reviewer provided constructive reviews. We especially thank Rodolfo Alito and his family for two months of generous hospitality, for permission to dig up their rice paddies, and for hiring and supervising laborers at the site.

References

Alexander, E. B., and N. Holowaychuk (1983). Soils on terraces along the Cauca River, Colombia. I. Chronosequence characteristics, *Soil Sci. Soc. Am. J.* **47,** 715–721.

Alvir, A. D. (1929). A geological study of the Angat-Novaliches region, *Philippine J. Sci.* **40,** no. 3, 359–419.

Arcilla, C. A. (1983). Geology and mineral resources of the Montalban Quadrangle, Luzon Philippines, Philippine Council for Agricultural and Resources Research Development, National Institute of Geological Sciences, unpublished report, 188 pp.

Arcilla, C. A., H. B. Ruelo, and J. Umbal (1989). The Angat ophiolite, Luzon, Philippines: lithology, structure, and problems in age determination, *Tectonophysics* **168,** 127–135.

Aurelio, M. A., E. S., Pagado, and H. J. Tebar (1993). Kinematics of the Philippine fault system at the Tongonan geothermal field, N. Leyte: implications for geothermal exploration and development, *J. Geol. Soc. Philippines* **67,** 1–20.

Barrier, E., P. Huchon, and M. A. Aurelio (1991). Philippine fault: a key for Philippine kinematics, *Geology* **19,** 31–35.

Birkeland, P. W. (1999). Soils and Geomorphology, Third Ed., Oxford University Press, New York, 448 pp.

Bullard, T. F., S. G. Wells, T. W. Gardner, N. Pinter, and R. L. Slingerland (1988). Geomorphic and pedogenic evolution of an emergent coastal piedmont, Osa Peninsula, Costa Rica: implications for latest Quaternary tectonism and fluvial adjustments, *Geol. Soc. Am., Abstracts with Programs* **20,** no. 7, A55.

Daligdig, J. A., H. Sato, T. Nakata, N. M. Tuñgol, and T. Nakamura (1994). Trenching activity along the Digdig fault, central Luzon, Philippines, in *Proc. of the Workshop on Paleoseismology, U.S. Geol. Surv. Open-File Rep. 94–568,* 43.

Defant, M. J., J. Z. de Boer, D. Oles (1988). The Geochemistry and tectonic setting of the Western Central Luzon Volcanic Arc, The Philippines: two arcs divided by rifting? *Tectonophysics* **145,** 305–307.

Dolan, J. E., K. Sieh, T. K. Rockwell, P. Guptill, and G. Miller (1997). Active tectonics, paleoseismology, and seismic hazards of the Hollywood fault, northern Los Angeles basin, California, *Geol. Soc. Am. Bull.* **109,** 1595–1616.

Förster, H., D. Oles, U. Knittel, M. J. Defant, and R. C. Torres (1990). The Macolod corridor: a rift crossing the Philippine island arc, *Tectonophysics* **183,** 265–271.

Garcia, L. C., R. G. Valenzuela, and T. G. Macalingcaq (1985). Catalog of Philippine earthquakes, Part A 1589–1864, in *Series on Seismology: Philippines,* E. P. Arnold (Editor), Vol. 6, Southeast Asia Association of Seismology and Earthquake Engineering, published under grant to the U.S. Geological Survey from the Office of Foreign Disaster Assistance, U.S. Agency for International Development, 1–57.

Gervasio, F. C. (1968). The geology, structures, and landscape development of Manila and suburbs: *Philippine Geologist* **22,** no. 4, 178–192.

Holzer, T. L. (1995). The 1995 Hanshin-Awaji (Kobe), Japan, earthquake, *GSA Today (Geol. Soc. Am.)* **5,** no. 8, 154–167.

Irving, E. M. (1947). Geomorphological implications of the Marikina drainage pattern, Rizal Province, Luzon, P.I., *Philippine Geologist* **1,** no. 2, 1—4.

Kelsey, H. M., A. G. Hull, S. M. Cashman, K. R. Berryman, P. H. Cashman, J. H. Trexler, Jr., J. G. Begg (1998). Paleoseismology of an active reverse fault in a forearc setting: the Poukawa fault zone, Hikurangi forearc, New Zealand, *Geol. Soc. Am. Bull.* **110,** 1123–1148.

Kelson, K. I., G. D. Simpson, W. R. Lettis, and C. C. Haraden (1996). Holocene slip rate and earthquake recurrence of the northern Calaveras fault at Leyden Creek, northern California, *J. Geophys. Res.* **101,** no. B3, 5961–5975.

Lienkaemper, J. L., and G. Borchardt (1996). Holocene slip rate of the Hayward fault at Union City, California, *J. Geophys. Res.* **101,** no. B3, 6099–6108.

Markewich, H. W., W. C. Lynn, M. J. Pavich, R. G. Johnson, and J. C. Meetz (1988). Analyses of four inceptisols of Holocene age, east-central Alabama, *U.S. Geol. Surv. Bull. 1589, C1–C29.*

McCalpin, J. P., Ed. (1996). *Paleoseismology,* Academic Press, Orlando, 588 pp.

Nakata, T., A. Sangawa, and S. Hirano (1977). A report on tectonic landforms along the Philippine fault zone in Northern Luzon, Philippines, Science Reports of the Tohoku University, Seventh Series (Geography), 7, 69–93.

PHIVOLCS Quick Response Teams (1994). 15 November 1994 Mindoro earthquake: preliminary report of investigation, Department of Science and Technology, Philippine Institute of Volcanology and Seismology, PHIVOLCS Special Report No. 2, 36 pp.

Punongbayan, R. S., R. E. Rimando, J. A. Daligdig, G. M. Besana, A. S. Daag, T. Nakata, and H. Tsutsumi, (1995). The 16 July 1990 Luzon earthquake ground rupture, Philippine Institute of Volcanology and Seismology, Technical Monograph, 1–32.

Punongbayan, R. S., J. A. Daligdig, G. M. Besana, N. M. Tuñgol, and R. E. Rimando (1996). The Marikina Valley fault system: active faulting in the eastern Metro Manila area, report of the Philippine Institute of Volcanology and Seismology submitted as a journal paper to the Philippine Journal of Volcanology and Seismology, 36 pp.

Repetti, W. C. (1946) Catalog of Philippine Earthquakes, *Bull. Seism. Soc. Am.* **36,** 133–322.

Rimando, R. E., R. S. Punongbayan, N. M. Tuñgol, H. T. Mirabueno, A. R. Nelson, and S. F. Personius (1995). Recent activity, kinematics and regional tectonic setting of the Marikina Valley fault system (MVFS), GEOCON '95, Eighth Annual Geological Convention of the Geological Society of the Philippines, Diliman, Quezon City, Philippines, Programme and Abstracts, p 21–22.

Ringenbach, J. C., N. Pinet, J. F. Stephan, and J. Delteil (1993). Structural variety and tectonic evolution of strike-slip basins related to the Philippine fault system, northern Luzon, Philippines, *Tectonics* **12,** 187–203.

Smith, W. D. (1924). Geology and Mineral Resources of the Philippine Islands, Philippine Bureau of Science Publication No. 19, Manila, 63 pp.

Serva, L., and D. B. Slemmons, Eds. (1995). Perspectives in paleoseismology, Association of Engineering Geologists Special Publication No. 6, Seattle, 139 pp.

Stuiver, M., and P. J. Reimer (1993). Extended ^{14}C data base and revised CALIB 3.0 ^{14}C age calibration program, *Radiocarbon* **35,** 215–230.

Thenhaus, P. C., S. L. Hanson, and S. T. Algermissen (1994). Estimates of the regional ground-motion hazard in the Philippines, in *Proc. of the National Conf. on Natural Disaster Mitigation,* Manila, Philippines, October, 28 pp.

U.S. Geological Survey (1996). USGS Response to an urban earthquake, *U.S. Geol. Surv. Open-File Report 96–263* (prepared for the Federal Emergency Management Agency), 81 pp.

Weldon, R. J. II, J. P. McCalpin, and T. K. Rockwell (1996). Paleoseismology in strike-slip tectonic environments, in *Paleoseismology,* J. P. McCalpin (Editor), Academic Press, Orlando, 271–329.

Wells, D., and K. J. Coppersmith (1994). New empirical relationships among magnitude, rupture length, rupture width, rupture area, and surface displacement, Bull. Seism. Soc. Am. **84,** 974–1002.

Wolf, J. A., and S. Self (1983). Structural lineaments and Neogene volcanism in southwestern Luzon, in *The Tectonic and Geologic Evolution of Southeast Asian Seas and Islands,* Part 2, D. E. Hayes (Editor), American Geophysical Union Geophysical Monograph 27, 157–172.

Yeats, R. S., and C. S. Prentice (1996). Introduction to special section: Paleoseismology, *J. Geophys. Res.* **101,** no. B3, 5847–5853.

Geologic Hazards Team, Central Region
U.S. Geological Survey, MS 966
PO Box 25046
Denver, Colorado 80225, USA
(A.R.N. and S.F.P.)

Philippine Institute of Volcanology and Seismology
University of the Philippines Campus
Diliman, Quezon City, The Philippines
(R.E.R., R.S.P., N.T., H.M., and A.R.)

Manuscript received 5 January 1999.